CHALMERS

Chalmers Publication Library

Coded Modulation for Fiber-Optic Networks

(article starts on next page)

Coded Modulation for Fiber-Optic Networks

Lotfollah Beygi, Erik Agrell, Joseph M. Kahn, Fellow, IEEE, and Magnus Karlsson

Abstract

In this tutorial, we study the joint design of forward error correction and modulation for fiber-optic communications. To this end, we use an information-theoretic design framework to investigate coded modulation (CM) techniques for standard additive white Gaussian noise channels and fiber-optic channels. This design guideline helps us to provide a comprehensive overview of the CM schemes in the literature. Then, by invoking recent advances in optical channel modeling for non-dispersion-managed links, we discuss two- and four-dimensional CM schemes. Moreover, we discuss the electronic computational complexity and hardware constraints of CM schemes for optical communications. Finally, we address CM schemes with signal shaping and rate-adaptation capabilities to accommodate the data transmission scheme to optical links with different signal qualities.

I. INTRODUCTION

The tremendous growth in the demand for high data rates in optical networks encourages exploiting the available resources in this medium more efficiently. A lot of efforts have been devoted to quantifying fundamental limits of fiber-optic channels [1]–[3]. Indeed, the more severe signal-dependent nonlinear effect in fiber-optic channels, compared to wireline and wireless channels, makes the channel modeling and capacity analysis of these channels cumbersome. The recent progress in channel modeling [4]–[6] and capacity analysis [3] of fiber-optic channels have opened a new horizon in the design of data transmission schemes operating with higher spectral efficiencies than current systems. The transparent reach, i.e., the transmission distance of a fiber-optic link with no inline electrical signal regenerators, is intimately related to the desired spectral efficiency, i.e., the number of information bits sent in each polarization per symbol

Lotfollah Beygi was with Chalmers University of Technology, Sweden, and is now with Qamcom Research & Technology AB, E-mail: beygi@qamcom.se. Erik Agrell and Magnus Karlsson are with Chalmers University of Technology, Sweden. E-mail: agrell, and magnus.karlsson@chalmers.se. Joseph M. Kahn is with Stanford University, USA. E-mail: jmk@ee.stanford.edu.

period, as well as to the digital signal processing (DSP) complexity (depicted in Fig. 1(a)). For example, the larger the transparent reach is, the higher the DSP complexity gets, provided that the desired spectral efficiency is achievable for this transparent reach.

Joint coding and (multilevel) modulation schemes, so-called coded modulation (CM), have been investigated as means to provide higher coding gain to increase reach, while maintaining acceptable complexity. The CM techniques [7] are known to be superior to conventional approaches using independent forward error correction (FEC) and modulation, in the sense of requiring less signal-to-noise ratio (SNR) for the same spectral efficiency. In fact, a CM scheme can exploit the four available dimensions of a fiber-optic link, i.e., two polarizations each consisting of in-phase and quadrature dimensions, with more flexibility than conventional schemes. In addition, the channel state information (CSI) can be taken into account in the design of a CM scheme, leading to a channel-aware CM scheme capable of adapting to different signal qualities in optically switched mesh networks with a dynamic or heterogeneous structure.

II. FIBER-OPTICAL LINKS

Light is an electromagnetic wave, which can be modulated to convey information bits in fiber-optic links including N spans, each consisting of a single mode fiber (SMF) and an erbium-doped fiber amplifier (EDFA). The electric field of the propagating signal experiences four types of impairments in these links: (i) signal attenuation, (ii) AWGN noise added in each EDFA after amplifying the signal to compensate for the fiber loss, (iii) frequency-dependent phase shift known as chromatic dispersion, and (iv) intensity-dependent phase shift in the time domain, the so-called nonlinear Kerr effect. If the fiber is broken into sufficiently short segments, the chromatic dispersion and the nonlinear Kerr effect can be thought of as acting sequentially and independently. The propagation of light in these channels is described by the nonlinear Schrödinger equation. Due to the lack of analytical solutions and the complexity of numerical approaches, deriving the discrete-time statistics of such channels is in general cumbersome.

A fiber-optic link can compensate for the chromatic dispersion optically using an inline dispersion compensation fiber, leading to a dispersion-managed link, or electronically by an electronic dispersion compensation (EDC) unit in the receiver, resulting in a so-called non-dispersion-managed (non-DM) link. Generally speaking, the high accumulated chromatic dispersion in a non-DM link turns the distribution
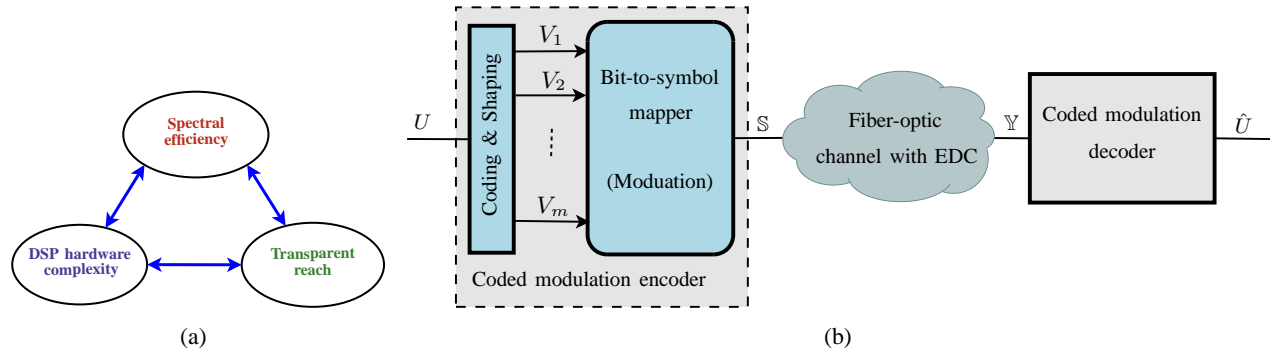
Fig. 1. (a) Three main factors in the design of a CM scheme for fiber-optic links. (b) A fiber-optic link including a CM encoder and decoder with EDC (U and $\hat{U}$ are the transmitted and decoded information bit sequences, respectively).

of the electric field into Gaussian and consequently mitigates the nonlinear Kerr effect. Therefore, non-DM links outperform the widely used dispersion-managed links for sufficiently large symbol rates and Gaussian or Nyquist pulses. The better performance of non-DM links has attracted a global interest in exploiting SMF links with EDC for next generation optical networks.

A non-DM link including a CM encoder and decoder with EDC is depicted in Fig. 1(b). As seen, the CM scheme first encodes the sequence of information bits U to m bit sequences V_1, V_2, ..., V_m. These m sequences are mapped to a sequence of symbols $\mathbb{S}$ from a 4D constellation (at each time instant, a vector consisting of one bit from each m bit sequences is mapped to a 4D symbol). A 4D constellation can be constructed by a Cartesian product of two equal quadrature amplitude modulations (QAM), which are used for independent data transmission over each polarization. The symbol sequence $\mathbb{S}$ is transmitted through a fiber-optic channel and received as the symbol sequence $\mathbb{Y}$ after the EDC.

A. Channel Model

Recently, a series of analytical models have been proposed for non-DM fiber-optic links [5], [6] with standard M-ary QAM (M-QAM) considering additive, Gaussian noise. The Gaussian noise model represents the received signal $\mathbb{Y}$ in a polarization-multiplexed (PM) fiber-optic channel with EDC as $\mathbb{Y} = \zeta\mathbb{S} + \mathbb{Z}$, where $\mathbb{S}$ is the transmitted PM signal, $\mathbb{Z}$ is a noise vector with a complex zero-mean circularly symmetric AWGN in each polarization, and ζ is a complex constant attenuation factor, which attenuates and rotates the transmitted symbol in each polarization. The variance of the zero-mean AWGN

TABLE I
SYSTEM PARAMETER VALUES

Symbol rate R_s	32 Gbaud
Nonlinearity coefficient γ	1.4 W^{-1}km^{-1}
Attenuation coefficient α	0.2 dB/km
Dispersion coefficient D	17 ps/nm/km
Optical center wavelength λ	1550 nm
EDFA noise figure F_n	5 dB
Span length L	80 km

in each polarization is given by $\sigma^2 = N\sigma^2_{\text{ASE}} + \sigma^2_{\text{NL}}$, where $\sigma^2_{\text{NL}} = a_{\text{NL}}P^3$ is the variance of the noise-like interference, the so-called nonlinear noise, caused by the nonlinear Kerr effect, in which a_{NL} is a function of channel parameters and P is the average transmitted power. The term $N\sigma^2_{\text{ASE}}$ denotes the variance of the total amplified spontaneous emission (ASE) noise from the EDFAs over N amplifier spans. Finally, the SNR is defined as $|\zeta|^2 P/\sigma^2$ for the non-DM system. Since the variance of the (nonlinear distortion) noise grows as the cube of the transmitted power, as shown in Fig. 2(a), the system performance is eventually degraded at high transmitted power levels. This nonlinear behavior distinguishes these channels from classical AWGN channels. Clearly, there is an optimum power (shown by two stars in Fig. 2(a)), which yields the minimum uncoded symbol error ratio (SER) or the maximum SNR after the EDC.

This optimum signal power is almost independent of the transparent reach and the systems introduced in this paper are assumed to operate at the optimal transmit power. A well-designed CM scheme allows for reliable data transmission with a higher uncoded SER, which leads to increasing the transparent reach. In this paper, we consider only a single-channel system, in order to keep the numerical simulation run time reasonable. However, the Gaussian noise model applies also to wavelength-division-multiplexing systems, as long as one accounts for the entire optical signal spectrum as outlined in, e.g., [5]. According to this model for non-DM fiber-optic links, numerically and experimentally validated, including effects of interchannel nonlinearities in the WDM case only increases the variance of the AWGN. This leads to a reduction in the maximum transparent reach at which a given bit rate can be achieved, but the results will not change qualitatively.
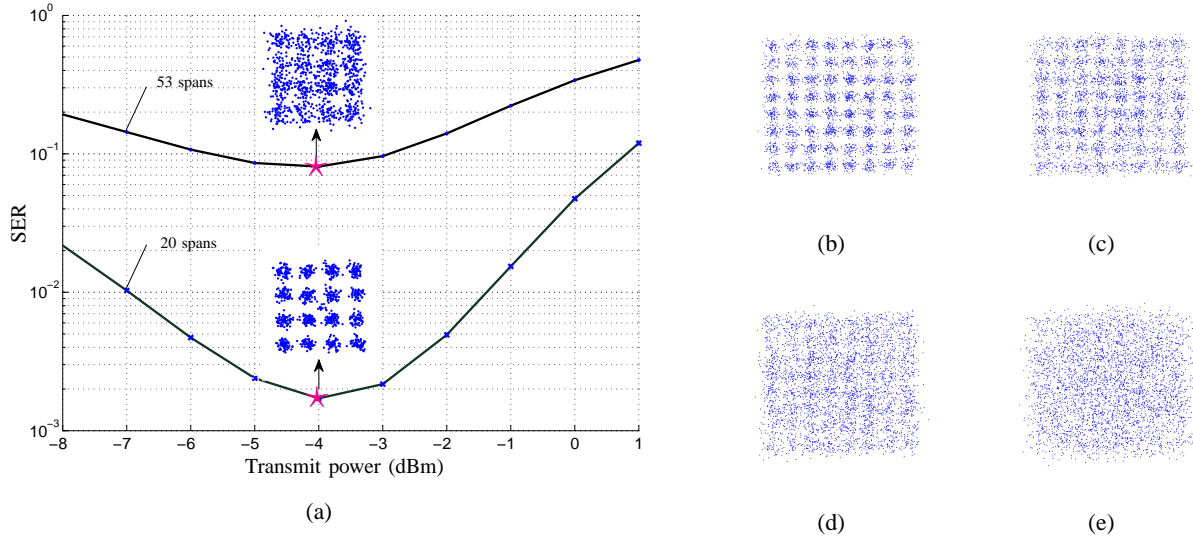
Fig. 2. (a) The SERs of a nonlinear fiber-optic link with 20 and 53 spans together with the scatter plots of the received signals for a 16-QAM at the minimum SER, marked by two stars. The scatter plot of the received signal for a nonlinear fiber-optic link with 64-QAM operating (b) 6.5 (c) 4.5 (d) 2.5 (e) 0 dB away from the AWGN channel capacity at a spectral efficiency of 5.5 bits per polarization. The values of the system parameters are given in Table I.

B. Quality Parameters

We will use three quality parameters to evaluate the performance of optical data transmission systems with hard- and soft-decision decoding, including FEC threshold, net coding gain (NCG), and gap to the AWGN channel capacity. These will be discussed separately below.

1) FEC threshold: Traditionally, due to the use of independent FEC and modulation together with hard-decision demodulation, the maximum bit error ratio (BER) of a hard-decision demodulator (the input BER of the FEC decoder), the so-called FEC threshold, for obtaining the information BER of 10^{-15} at the output of the FEC decoder has been widely used as a metric for these channels. Often, the main goal of system designers was to meet the desired FEC threshold for an uncoded system.

2) Net coding gain: The reduction in the SNR requirement resulting from adding coding at the same information bit rate and the same (low) information BER for both coded and uncoded systems is called the net coding gain (NCG). The code rate of the coded system is $R = \eta_{\text{uncod}}/\eta$, where η_{uncod} and η are the spectral efficiencies of the uncoded and coded systems, respectively. The system coding overhead is defined as $\text{OH} = 1/R - 1$. The NCG is precisely defined as the gross coding gain scaled by the code rate of the coded system to compare the coded and uncoded systems at the same information bit rate

[8]. The NCG of a system at a certain information BER can be expressed as NCG $= R\gamma_{\text{uncod}}/\gamma$, where γ_{uncod} and γ are the SNRs required to meet the desired BER for the given uncoded and coded systems, respectively.

3) Gap to the AWGN channel capacity: The advent of CM schemes in fiber-optic communications with soft-decision decoding enables new evaluation techniques for these systems. For a system with a rate R, there is a minimum SNR γ (in dB) to obtain a BER of 10^{-15} at the output of the CM decoder, which is usually computed by numerical simulations. The gap $\Delta\gamma$ between γ and the minimum SNR obtained using the Shannon formula for an AWGN channel with the spectral efficiency η, i.e., $2^\eta - 1$, is a useful measure to compare different CM schemes[1]. This gap, known as gap from AWGN capacity [9], can be expressed as $\Delta\gamma = \gamma - 10\log_{10}(2^\eta - 1)$ dB. In Fig. 2(b)–(e), we have shown the scatter plots of the received signal for a non-DM fiber-optic link with 10, 15, 23, and 39 spans and the system parameters given in Table I, operating at 6.5, 4.5, 2.5, and 0 dB, resp., from the AWGN channel capacity.

III. CM TECHNIQUES

Considering the bit-to-symbol mapper shown in Fig. 1(b), the equivalent binary subchannels approach introduced in [10] can be applied to represent the mutual information (MI) between the channel input and the received signal after EDC as $I = \sum_{i=1}^{m} I_i$, where $I_i = I(V_i; \mathbb{Y}|V_1, \ldots, V_{i-1})$ is the conditional MI of subchannel i, provided that the transmitted bits of the subchannels $1, \ldots, i-1$ are given. The detection of the channel input bits is performed with a multistage decoder. An accurate channel model (see Section II-A) is necessary to exploit this design framework. More precisely, this information-theoretic tool requires the signal statistics of the received signal $\mathbb{Y}$ from the channel. Clearly, the channel with input $\mathbb{S}$ and output $\mathbb{Y}$ can be modeled as m parallel subchannels with the inputs V_i, $i = 1, \ldots, m$ and the output $\mathbb{Y}$. An alternative parallel subchannel modeling approach is based on decoding the individual subchannels independently [10], which yields a sum rate of $\hat{I} = \sum_{i=1}^{m} \hat{I}_i$, in which $\hat{I}_i = I(V_i; \mathbb{Y})$. It can be shown that $I(V_i; \mathbb{Y}) \leqslant I(V_i; \mathbb{Y}|V_1, \ldots, V_{i-1})$ [10], implying that $\hat{I} < I$. The gap between $\hat{I}$ and

---

[1]The AWGN capacity, although popular as a benchmark, may not represent the capacity of the nonlinear fiber-optic channel [3].

Fig. 3. Concatenation of an outer (RS or BCH) and inner (CM scheme) codes.

I strongly depends on the selected labeling of the constellation symbols. This gap is surprisingly small with Gray labeling. However, the multistage decoding technique is significantly superior to the parallel independent decoding for a finite-length code [10]. We explain below the three main categories of CM schemes, exploiting the equivalent subchannels for AWGN channels, as well as two CM schemes that are constructed from nonbinary component codes. They are all illustrated in Fig. 4.

As shown in Fig. 3, the CM schemes may be concatenated with an outer code to solve the problem of finding a coded scheme that has both a rapidly decreasing BER at moderate SNR, known as the waterfall region, and the possibility of reaching extremely low BERs without any error floor [11, Ch. 5]. As suggested in [8], one may use a capacity-approaching inner code, here realized by a CM scheme, to obtain BERs around 10^{-3}. Then the BER floor is suppressed using an outer code constructed based on classic codes with hard-decision decoding such as RS or BCH codes to BERs acceptable for optical communications, e.g., 10^{-15}. The distributions of the received 2D or 4D symbols before decoding are computed using the noise variance given in Section II-A.

A. Multilevel Coded Modulation (MLCM)

For an arbitrary modulation, the binary subchannels have in general different conditional MIs I_i. Hence, to approach the channel MI I, an unequal error protection technique, as depicted in Fig. 4 (a), is applied over the m binary subchannels. To this end, MLCM was designed consisting of m binary turbo [10] or LDPC [12] codes, originally introduced with classic block codes [13], each adapted to the conditional MI of the corresponding subchannels (I_i for channel i). MLCM has been shown to be a capacity-achieving scheme theoretically and through simulations [10] for AWGN. An interesting feature of MLCM is the possibility of exploiting a multistage decoder (MSD). As shown in Fig. 4 (a), the decoder of the first subchannel can decode the received bits independently of the other subchannels, then the second decoder uses the output from the first decoder to decode the bits received in the second subchannel, and so on for

(a) MLCM

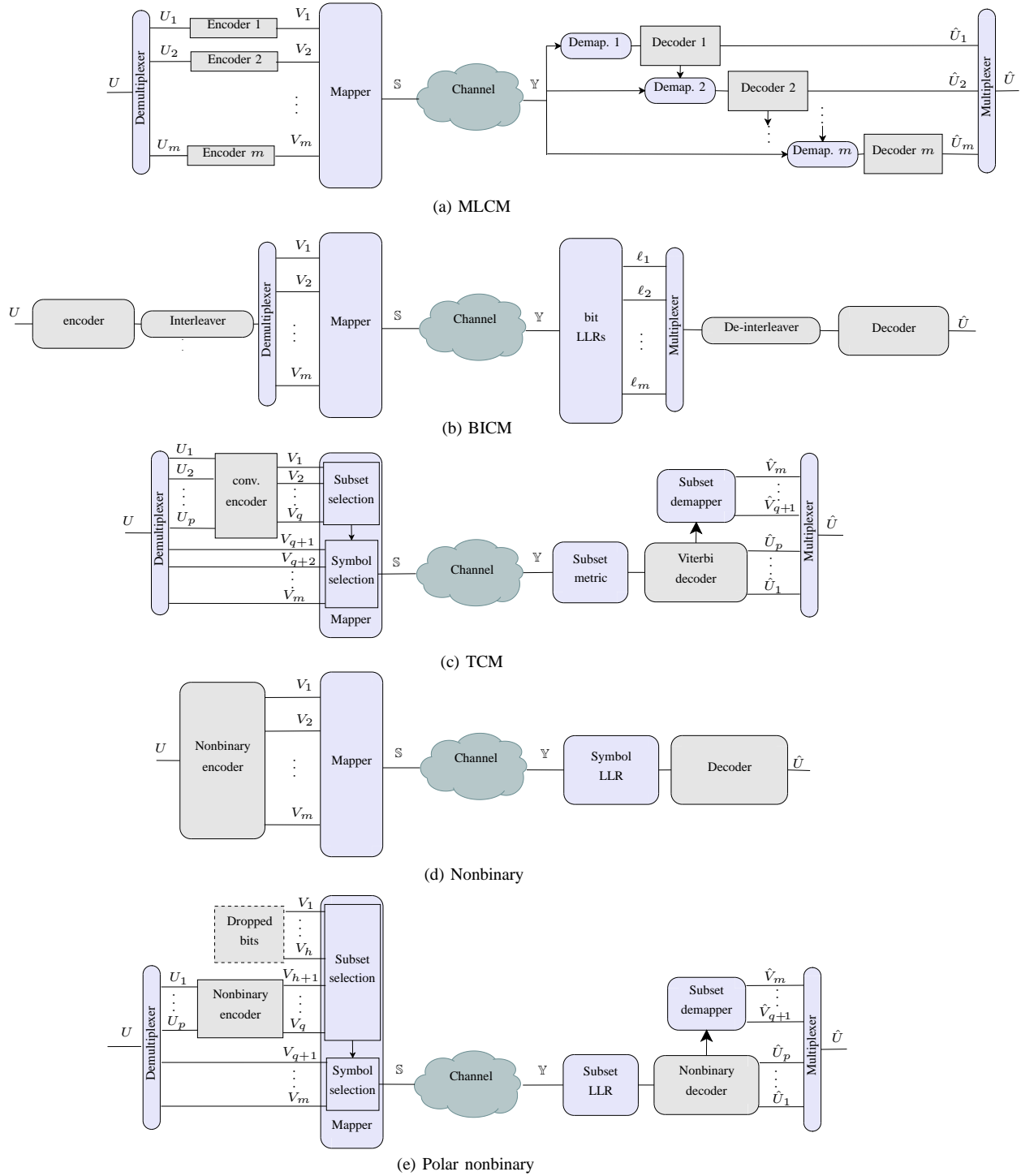(b) BICM

(c) TCM

(d) Nonbinary

(e) Polar nonbinary

Fig. 4.   The block diagram of CM schemes: (a) MLCM (b) BICM (c) TCM (d) Nonbinary (e) Polar nonbinary.

the rest of the subchannels. The MSD has lower complexity than the maximum-likelihood detector. An MLCM scheme was tailored in [14] for a memoryless nonlinear fiber-optic channel with RS component codes. In this paper, an unequal error protection scheme in the phase and radial direction of a 16-point ring constellation is exploited to minimize the block error rate of the system. For non-DM fiber-optic channels, two simplified MLCM schemes were introduced in [15] with staircase codes and LDPC codes, respectively. The subchannels are categorized in two groups in [15] and three groups in [16], to reduce the number of component codes.

B. Bit-Interleaved Coded Modulation (BICM)

Zehavi [17] introduced BICM as shown in Fig. 4 (b) simply by adding an interleaver between the encoder and the mapper to distribute the coded bits among different binary subchannels uniformly and exploit the diversity in the subchannels. In the BICM scheme, the subchannels are assumed to be independent and a simplified model using m independent decoders of the binary subchannels is used [10] with the MI $I(V_i; \mathbb{Y})$ for subchannel $i = 1, \ldots m$, in which each subchannel has no information from the input bits of the other subchannels. Usually, the binary decoder uses the log-likelihood ratios (LLR) of the subchannels after de-interleaving to decode the received bits, where the LLR of bit v is defined as $\ln \big(\Pr(v = 1|\mathbb{Y}) / \Pr(v = 0|\mathbb{Y}) \big)$.

For channels such as wireless fast fading channels, the channel is unknown at the transmitter, and thus, the MIs of the subchannels are also unknown. BICM was originally proposed for fast fading channels to exploit the diversity in binary subchannels [10]. BICM has been widely investigated in fiber-optic communications. For example, a comprehensive study of BICM for fiber-optic communications has been performed in [18] with different modulation formats. The performance of a BICM scheme is very sensitive to the type of the selected constellation labeling. Its performance is significantly degraded for a non-Gray labeling. To overcome this problem, one may exploit an iterative decoding between the 2D or 4D demapper (LLR calculation unit) and the binary code decoder [19].

C. Trellis-Coded Modulation (TCM)

Ungerboeck [20] introduced a new type of binary labeling based on the set partitioning technique. The subchannels resulting from this labeling have ascending MI values. The early subchannels (with smaller indices) have lower MI values than the subchannels with indices close to m. The original version of TCM, shown in Fig. 4 (c), splits the information bits into two groups of subchannels, where the group with smaller indices, the so-called "subset selection," is protected by a convolutional code, while the second group, denoted as "symbol selection," remains uncoded. Although this scheme can be decoded by MSD, Ungerboeck proposed a maximum likelihood decoder. The Viterbi decoder uses the subset metrics to decode the first group. The second group is decoded by a simple demapper within the decoded subset.

A capacity-approaching TCM scheme, known as turbo TCM, can be designed by replacing the convolutional code with a turbo code to decrease the gap from the Shannon limit for AWGN channels. Furthermore, multidimensional TCM was proposed in [21], which allows a higher spectral efficiency for a given signal constellation than one-dimensional (1D) or 2D TCM methods. In fiber-optic systems, TCM was proposed in [22] with an 8-point cubic polarization shift keying constellation. The simplest 4- and 16-state TCM schemes were applied to 8-point phase shift keying (PSK) and differential PSK in [23]. Finally, the concatenation of 2D TCM with two different outer codes, RS and BCH codes, was studied in [24], which gives NCGs of 8.4 and 9.7 dB, respectively, at a BER of 10^{-13} for the AWGN channel.

D. CM Scheme with a Nonbinary Block Code

The codewords of a nonbinary code are sequences of 2^q-ary symbols, each representing q bits. The code is constructed over a Galois field (GF) of order 2^q, denoted by GF(2^q). Binary codes can be considered as the simplest case of these codes, defined over GF(2) with two symbols 0 and 1. The binary subchannels can be encoded and decoded jointly using nonbinary codes, at the cost of increased complexity. As shown in Fig. 4 (d), the demapper computes symbol LLRs for each soft received symbol, retaining the MI between the subchannels compared to the independent bit LLR calculation in BICM. In fact, since symbol-wise decoding is used for a nonbinary scheme, its performance is not sensitive to the type of the selected constellation labeling and the decoding is performed with no iteration between the LLR

calculation unit and the CM decoder.

Different types of nonbinary codes such as classic nonbinary codes, e.g., RS codes with a hard-decision decoding, or modern nonbinary LDPC and turbo TCM codes with a soft-decision decoding, can be used to construct the nonbinary CM schemes. Moderate-length (< 2000 GF symbols) nonbinary LDPC codes have been widely proposed for fiber-optic communications [25], to approach the Shannon limit in AWGN channels. The nonbinary scheme can be used with both 2D [25] and 4D [16], [26] constellations.

E. Polar nonbinary CM Scheme

Although many techniques have been suggested to mitigate the computational complexity of nonbinary codes, the decoding complexity in the order of $O(q2^q)$, for a regular nonbinary LDPC code designed over GF(2^q), makes this scheme unrealistic for large ($\geq 2^7$ points) constellations [27]. To overcome this problem, a mapper, inspired by the polar coding technique [28], was devised [16] to categorize the binary subchannels into three groups, namely 'bad,' 'intermediate,' and 'good' subchannels. The 'bad' and 'good' subchannels have MIs near 0 and 1, respectively, while the MIs of 'intermediate' subchannels are between 0 and 1. Then, error protection using nonbinary LDPC coding is performed solely over the 'intermediate' subchannels. As shown in Fig. 4 (e), the 'good' subchannels are left uncoded, whereas no information is transmitted on the 'bad' subchannels denoted by dropped bits, which are fixed to zero and known to the receiver. Since the nonbinary encoder performs on the 'intermediate' subchannels independently of the constellation size [16], the GF can have a lower order with this design than with the regular nonbinary scheme above, and consequently a CM scheme with a lower complexity is obtained. In this scheme, the bit-to-symbol mapper can be realized by a 4D set partitioning technique illustrated using the bits $V_1, \ldots, V_4$ in Fig. 5 for a PM-QPSK constellation [16].

IV. 2D VERSUS 4D CM SCHEMES

A CM scheme can exploit the available four dimensions in the signal space of a fiber-optic link either jointly as a 4D channel or separately as two parallel 2D channels. For the Gaussian noise model introduced in Section II-A, these parallel channels are independent, as shown in [10], and one can get
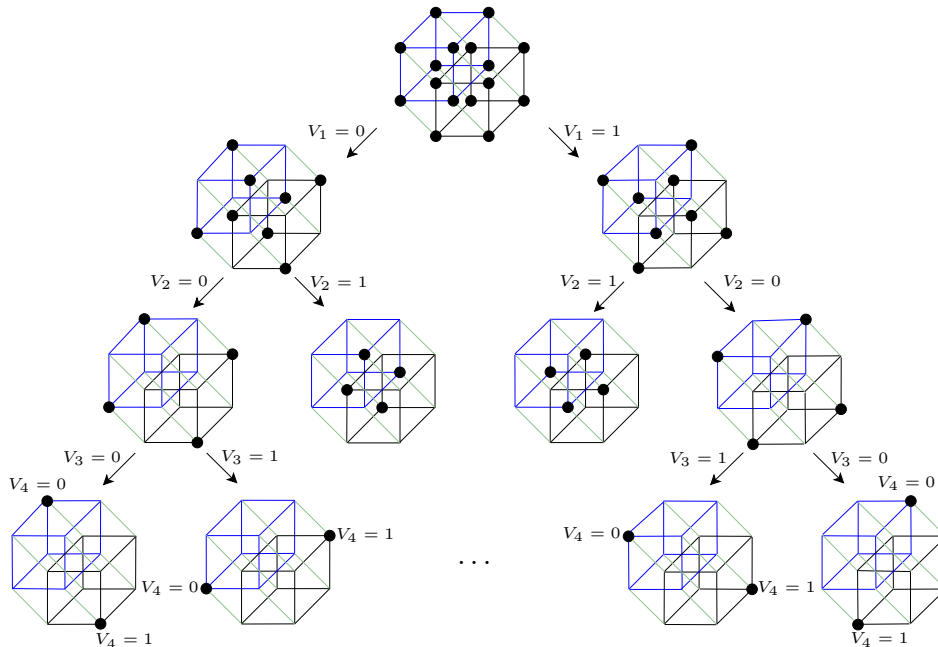
Fig. 5. 4D set partitioning of a 16-ary 4D constellation representing PM-QPSK. $V_4V_3V_2V_1$ represents the four bits in the binary labeling of the constellation [16].

close to the MI of an AWGN channel using both 1D and 2D schemes. Although a 2D CM scheme can achieve the MI of AWGN channels, a 4D CM scheme has a better trade-off between complexity and performance at the same spectral efficiency, as shown later in the performance analysis (see Section VI). In fact, a 4D scheme can provide more flexibility than 1D or 2D schemes, which facilitates exploiting rate adaptation and probabilistic shaping techniques. Here, we investigate 2D and 4D CM schemes with binary and nonbinary codes.

Classic and modern binary codes as well as their concatenations are used together with 2D constellations such as QAM signals for constructing 2D CM schemes. They are well investigated for fiber-optic communications and have been realized based on the three traditional CM schemes, i.e., MLCM [15], TCM [24], and BICM [18]. This group of CM schemes is capable of approaching the AWGN capacity provided that the block length is sufficiently large. For example, an NCG of 10.8 dB ($\Delta\gamma = 3$ dB) with 20.5% coding overhead is achieved with triple-concatenated codes, (4608, 4080) LDPC, (3860, 3824) BCH, and (2040, 1930) BCH using QPSK signals at a BER of 10^{-15} [8], where (n, k) denotes a block code with a codeword of length n bits and an input information vector of length k bits. As introduced

in [25], the 2D CM schemes can also be constructed using nonbinary codes. The (1225, 1088) LDPC code over GF(2^3) with 12.6% coding overhead provides an NCG of 9.4 dB ($\Delta\gamma = 2.3$ dB) at a BER of 10^{-10}. The improvement over the comparable binary (3136, 2800) LDPC code from the same family is 0.7 dB at a BER of 10^{-7}.

CM schemes with 4D constellations adopted from classical communication have been suggested for optical communications based on BICM. For example, a 4D BICM scheme with two concatenated codes, an outer (992, 956) RS code and an inner (9252, 7976) LDPC code, can provide an NCG of 10.5 dB ($\Delta\gamma = 2.7$ dB) at a BER of 10^{-13} with an overall coding overhead of 20% and QPSK constellation [19]. In Fig. 4 (d) and (e), nonbinary codes are applied to 4D CM schemes to improve the NCG of these systems, for example 0.29 dB, 1.17 dB, and 2.17 dB with 16-, 32-, and 64-point 4D constellations, respectively, at a BER of 10^{-7} [26]. The nonbinary scheme in Fig. 4 (d) suffers from high complexity for constellations with a large number of symbols ($\geq 2^7$). The polar nonbinary CM scheme in Fig. 4 (e) decreases the complexity of the nonbinary CM schemes without performance degradation, by confining the required GF order of the nonbinary block code to a small number ($< 2^7$ symbols), independent of the constellation size. Finally, it can be concluded that 4D schemes may be more spectrally efficient than 2D schemes at the same performance.

V. Hardware requirement and DSP processing complexity

The hardware requirements and electronic processing complexity of CM schemes play a crucial role for fiber-optic communications. Although the semiconductor technology is capable of providing ultra-high-speed analog-to-digital converters (ADC) and massively parallelized DSP circuits, the system power consumption and hardware cost also need to be taken into account. In particular, since high-resolution ADCs and DSPs are costly for high-speed data transmission, the performance sensitivity of CM schemes to quantization errors has become an important factor in the design of these schemes [8]. The impact of quantization errors on the performance of a concatenated TCM scheme with two interleaved BCH outer codes was evaluated in [24], and it was shown that 4-bit quantization was sufficient to approach the infinite-precision performance to within 0.15 dB.

The complexity of a CM scheme is dominated by its two main components: the LLR calculation from the soft received symbols and the encoder and decoder of the component codes. To compute the LLR vector for a 4D CM scheme, finding the closest 4D symbol to the received vector among the constellation symbols requires approximately 4 times the computational complexity of finding the closest 1D symbol in the constituent 1D constellation, neglecting the 3 additions which may be needed to compute the 4D minimum Euclidean distance from four 1D minimum Euclidean distances [21]. This implies that one may compare the complexity of the receivers for CM schemes with different dimensions by taking into account solely the complexity of the component code decoders per dimension.

The complexity of LDPC and RS codes has been well-studied in the literature. The computational complexity required per iteration of the fast Fourier transform sum-product algorithm in decoding a 2^q-ary regular nonbinary LDPC code designed over $GF(2^q)$ is in the order of $O(J\rho q 2^q)$, where J and ρ are the number and weight of the rows of the parity-check matrix of the nonbinary LDPC code, respectively. This complexity is in the order of $O(q^2 2^q)$ for RS codes [11, Ch. 14]. Moreover, the number of iterations required for the convergence of LDPC iterative decoding also influences the complexity of the decoder of these codes.

VI. PERFORMANCE ANALYSIS OF 2D AND 4D SCHEMES

We compare the BER performance for three CM schemes: 2D BICM, 2D nonbinary CM, and 4D polar nonbinary CM schemes, illustrated in Fig. 4 (b), (d), (e), respectively. All schemes were designed with PM 64-QAM and an overall coding overhead of 21% over a single-channel non-DM fiber-optic link with the system parameters given in Table I. The exploited LDPC codes were constructed based on finite fields [11, Ch. 11]. The numerical simulations of signal propagation in a non-DM fiber-optic link based on the Manakov equation are performed using the split-step Fourier method. Here, the schemes are compared based on two constraints: block length and complexity.

A. Block-length-constrained comparison

Three systems are simulated with the same transmission block length consisting of inner and outer codes together with an interleaver as shown in Fig. 3 for the following scenarios: (i) a 2D BICM scheme

with a (3, 21)-regular quasi-cyclic[2] binary (10752, 9236) LDPC inner code concatenated with a (1016, 980) shortened RS outer code over $GF(2^{10})$, to bring down the output BER of the inner code from 2.2×10^{-4} to 10^{-15}; (ii) a 2D nonbinary CM scheme with a (3, 9)-regular quasi-cyclic nonbinary (2688, 2309) LDPC inner code over $GF(2^6)$ concatenated with a (970, 930) shortened RS code over $GF(2^{10})$, to bring down the output BER of the inner code from 1.9×10^{-4} to 10^{-15}; (iii) a 4D polar nonbinary CM scheme with a (3, 9)-regular quasi-cyclic nonbinary (1728, 1162) LDPC inner code over $GF(2^6)$ concatenated with a (963, 949) shortened RS code over $GF(2^{10})$, to bring down the output BER of the inner code from 1.5×10^{-5} to 10^{-15}.

The length of the interleaver between the inner and the outer code is 11 times the inner code length for the 2D BICM and 7 times the inner code length for the 2D nonbinary CM schemes, resulting in coded block lengths of $11 \times 10752 = 118272$ and $7 \times 2688 \times 6 = 112896$ bits, respectively. The interleaver length is 5 times the inner code length for the 4D polar nonbinary CM scheme, resulting in a coded block length of $5 \times 1728 \times 12 = 103680$ bits. Considering transmission of 12 bits by each 4D symbol at 32 Gbaud, we obtain block lengths of 308, 294, and 270 ns for the 2D BICM, 2D nonbinary, and polar 4D nonbinary schemes, respectively. According to the BER results shown in Fig. 6(a), the polar 4D nonbinary scheme is superior to the 2D BICM and 2D nonbinary CM schemes with nearly the same transmission block length.

B. Complexity-constrained comparison

We designed the following 2D and 4D schemes with similar complexities using the results provided in Section V: (i) a 2D BICM scheme consisting of a (3, 21)-regular quasi-cyclic binary (16128, 13844) LDPC inner code concatenated with a (1015, 977) shortened RS outer code over $GF(2^{10})$, to bring down the output BER of the inner code from 2.3×10^{-4} to 10^{-15}; (ii) a 4D polar nonbinary CM scheme consisting of a (3, 9)-regular quasi-cyclic nonbinary (1152, 778) LDPC inner code over $GF(2^6)$ concatenated with a (1011, 995) shortened RS outer code over $GF(2^{10})$, to bring down the output BER of the inner code

---

[2]A (γ, ρ)-regular quasi-cyclic LDPC code has γ nonzero elements in each column and ρ nonzero elements in each row of its parity-check matrix [11, Ch. 5].
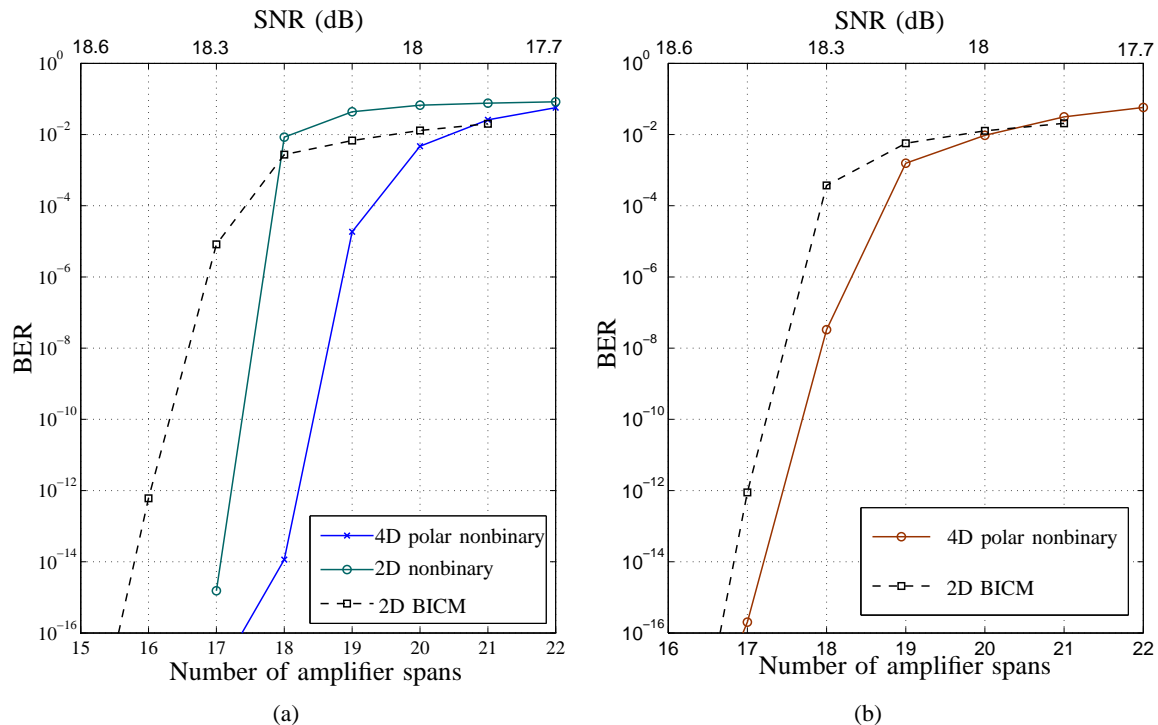
Fig. 6. (a) The BER of three CM schemes with information-block-length-constraint. (b) The BER of 2D and 4D CM schemes with binary and nonbinary LDPC codes, respectively and similar complexity. All the CM schemes use PM 64-QAM with 21% coding overhead and have therefore the same spectral efficiency.

from 2.5×10^{-5} to 10^{-15}. As seen in Fig. 6(b), the 4D polar nonbinary scheme performs slightly better. Since the GF order can be kept fixed in this scheme, i.e., $GF(2^6)$, independent of the constellation size, the 4D scheme is superior to the 2D scheme for large constellations.

VII. SIGNAL SHAPING

Signal shaping in data transmission systems over AWGN channels refers to the manipulation of the symbol distribution to make it better approximate a Gaussian distribution [7]. Two types of shaping methods have been proposed for optical communications: probabilistic [15], [16] and geometric [29] shaping. Probabilistic shaping means changing the symbol probabilities for a standard constellation such as QAM, while geometric shaping implies changing the coordinates of the points in the constellation, which typically results in irregular (nonuniform) constellations. Two well-established probabilistic shaping methods, shell mapping and trellis shaping [7], have been applied to fiber-optic communications in [16] and [15], respectively. With probabilistic shaping, instead of having a uniform distribution for the input
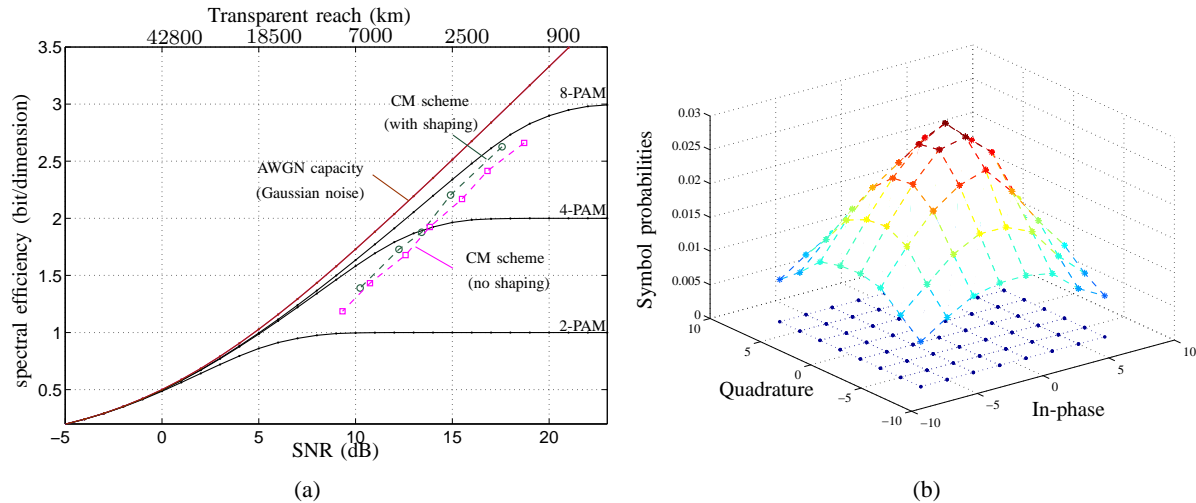
Fig. 7. (a) The spectral efficiency per dimension versus the transparent reach and the SNR for a non-DM link with EDC. The CM scheme curves are based on the results given in [16] and the spectral efficiency for the Gaussian noise model is computed by $\log_2(1 + \text{SNR})/2$, where $\text{SNR} = |\zeta|^2 P/\sigma^2$. (b) The 2D symbol probabilities of the probabilistically-shaped 4D CM scheme.

symbols, the symbols close to the origin of the constellation (with small amplitudes) are sent more often than the symbols far from the origin, as illustrated in Fig. 7(b) for a 64-QAM with the shell mapping algorithm. Probabilistic shaping reduces the average transmitted power compared with a uniform distribution. Bearing in mind that the variance of the introduced nonlinear distortion is cubic with input power (see Section II-A), the system performance improves by performing probabilistic shaping as shown in Fig. 7(a) [16].

VIII. RATE-ADAPTIVE CM SCHEMES

To improve the utilization of optical networks with dynamic or heterogeneous structure, the rate of the CM scheme can be adapted according to the CSI at the transmitter of each fiber-optic link. Two well-known choices for the CSI are (i) the SNR, which is estimated after EDC, and (ii) the inner code BER, which is computed by a syndrome-based error estimator [9]. Rate-adaptive schemes have been investigated using multiple codes with different rates or a single fixed-rate code [9], [16], [30]. Different code rate can be constructed either separately or by puncturing or shortening a single mother code. For example, a rate-adaptive nonbinary scheme with six nonbinary LDPC codes was proposed in [30] to provide a transmission bit rate between 100 Gb/s and 300 Gb/s in steps of 26.67 Gb/s at a fixed symbol

rate. In a more practical scenario, a rate-adaptive BICM scheme was proposed exploiting six combinations of binary LDPC and RS codes together with three modulations formats [9].

The method based on multiple codes with different rates is demanding in terms of hardware and thus costly to implement. A 4D scheme with a flexible structure can perform rate adaptation with a single component code rather than using a different code for each rate. The 4D scheme shown in Fig. 4(e) was used in [16] to devise a rate-adaptive scheme with a single fixed-rate encoder. In this scheme, the number of bits in the different 'good' and 'bad' groups introduced in the polar CM scheme in Section III-E are adjusted according to the CSI such that the number of 'intermediate' bits is always the same. Since the mapper is solely a simple look-up table, the rate adaptation is straightforward to implement. As shown in Fig. 7(a), the rate-adaptive CM scheme using a single nonbinary code with probabilistic shaping can achieve $\Delta\gamma < 3$ dB for transparent reaches from 17×80 to 112×80 km.

IX. Summary

To utilize the available resources in an optical network efficiently, the trade-off between spectral efficiency, DSP hardware complexity, and transparent reach needs to be optimized for different links in the network. Joint coding and modulation schemes offer more freedom to exploit the available four dimensions in these channels than traditional independent FEC and modulation techniques. As discussed, a CM scheme can operate over a link with larger transparent reach than conventional schemes but with the same complexity (or even lower), for a wide range of spectral efficiencies.

Among the CM schemes discussed for AWGN channels, namely, MLCM, BICM, TCM, nonbinary, and polar nonbinary schemes, MLCM is not attractive for fiber-optic communications because of its large number of component codes. The main bottleneck of nonbinary schemes is the decoding complexity, making it an unrealistic solution for large constellations. A better trade-off between DSP complexity and transparent reach of 4D CM schemes makes them superior to 2D schemes. Finally, a 4D CM scheme provides more flexibility than 1D and 2D CM schemes, which facilitates its combination with signal shaping techniques as well as rate adaptation methods with no need for multiple component codes.

REFERENCES

[1] R.-J. Essiambre, G. Kramer, P. J. Winzer, G. J. Foschini, and B. Goebel, "Capacity limits of optical fiber networks," *J. Lightwave Technol.*, vol. 28, no. 4, pp. 662–701, Feb. 2010.

[2] A. D. Ellis, J. Zhao, and D. Cotter, "Approaching the non-linear Shannon limit," *J. Lightwave Technol.*, vol. 28, no. 4, pp. 423–433, Feb. 2010.

[3] E. Agrell, "On monotonic capacity–cost functions," 2012. [Online]. Available: http://arxiv.org/abs/1108.0391

[4] A. Mecozzi and R.-J. Essiambre, "Nonlinear Shannon limit in pseudolinear coherent systems," *J. Lightwave Technol.*, vol. 30, pp. 2011–2024, Jun. 2012.

[5] P. Poggiolini, "The GN model of non-linear propagation in uncompensated coherent optical systems," *J. Lightwave Technol.*, vol. 30, no. 24, pp. 3857–3879, Dec. 2012.

[6] L. Beygi, E. Agrell, P. Johannisson, M. Karlsson, and H. Wymeersch, "A discrete-time model for uncompensated single-channel fiber-optical links," *IEEE Trans. Commun.*, vol. 60, no. 11, pp. 3440–3450, Nov. 2012.

[7] G. D. Forney, Jr. and G. Ungerboeck, "Modulation and coding for linear Gaussian channels," *IEEE Trans. Inform. Theory*, vol. 44, no. 6, pp. 2384–2415, Oct. 1998.

[8] F. Chang, K. Onohara, and T. Mizuochi, "Forward error correction for 100 G transport networks," *IEEE Commun. Mag.*, vol. 48, no. 3, pp. S48–S55, Mar. 2010.

[9] G.-H. Gho and J. M. Kahn, "Rate-adaptive modulation and low-density parity-check coding for optical fiber transmission systems," *J. Optical Commun. Netw.*, vol. 4, no. 10, pp. 760–768, Oct. 2012.

[10] U. Wachsmann, R. F. H. Fischer, and J. B. Huber, "Multilevel codes: theoretical concepts and practical design rules," *IEEE Trans. Inform. Theory*, vol. 45, no. 5, pp. 1361–1391, Jul. 1999.

[11] W. E. Ryan and S. Lin, *Channel Codes: Classical and Modern*. Cambridge University Press, 2009.

[12] J. Hou, P. Siegel, L. Milstein, and H. Pfister, "Capacity-approaching bandwidth-efficient coded modulation schemes based on low-density parity-check codes," *IEEE Trans. Inform. Theory*, vol. 49, no. 9, pp. 2141–2155, Sep. 2003.

[13] H. Imai and S. Hirakawa, "A new multilevel coding method using error correcting codes," *IEEE Trans. Inform. Theory*, vol. 23, pp. 371–377, May 1977.

[14] L. Beygi, E. Agrell, P. Johannisson, and M. Karlsson, "A novel multilevel coded modulation scheme for fiber optical channel with nonlinear phase noise," *in Proc. IEEE Global Commun. Conf.*, Dec. 2010.

[15] B. P. Smith and F. R. Kschischang, "A pragmatic coded modulation scheme for high-spectral-efficiency fiber-optic communications," *J. Lightwave Technol.*, vol. 30, no. 13, pp. 2047–2053, Jul. 2012.

[16] L. Beygi, E. Agrell, J. M. Kahn, and M. Karlsson, "Rate-adaptive coded modulation for fiber-optical communications," *J. Lightwave Technol.*, to appear, 2013.

[17] E. Zehavi, "8-PSK trellis codes for a Rayleigh channel," *IEEE Trans. Commun.*, vol. 40, no. 5, pp. 873–884, May 1992.

[18] I. B. Djordjevic, M. Arabaci, and L. L. Minkov, "Next generation FEC for high-capacity communication in optical transport networks," *J. Lightwave Technol.*, vol. 27, no. 16, pp. 3518–3530, Aug. 2009.

[19] H. Bülow and E. Masalkina, "Coded modulation in optical communications," *in Proc. Optic. Fiber Commun. Conf.*, Mar. 2011.

[20] G. Ungerboeck, "Channel coding with multilevel/phase signals," *IEEE Trans. Inform. Theory*, vol. 28, no. 1, pp. 55–67, Jan. 1982.

[21] L. F. Wei, "Trellis-coded modulation with multidimensional constellations," *IEEE Trans. Inform. Theory*, vol. 33, no. 4, pp. 483–501, Jul. 1987.

[22] S. Benedetto, G. Olmo, and P. Poggiolini, "Trellis coded polarization shift keying modulation for digital optical communications," *IEEE Trans. Commun.*, vol. 43, no. 234, pp. 1591–1602, Feb./Mar./Apr. 1995.

[23] H. Zhao, E. Agrell, and M. Karlsson, "Trellis-coded modulation in PSK and DPSK communications," *in Proc. European Conf. and Exhibition on Optic. Commun.*, Sep. 2006, We3.P.93.

[24] M. Magarini, R.-J. Essiambre, B. E. Basch, A. Ashikhmin, G. Kramer, and A. J. de Lind van Wijngaarden, "Concatenated coded modulation for optical communications systems," *IEEE Photon. Technol. Lett.*, vol. 22, no. 16, pp. 1244–1246, Aug. 2010.

[25] I. Djordjevic and B. Vasic, "Nonbinary LDPC codes for optical communication systems," *IEEE Photon. Technol. Lett.*, vol. 17, no. 10, pp. 2224–2226, Oct. 2005.

[26] M. Arabaci, I. Djordjevic, L. Xu, and T. Wang, "Four-dimensional non-binary LDPC-coded modulation schemes for ultra-high-speed optical fiber communication," *IEEE Photon. Technol. Lett.*, vol. 23, no. 18, pp. 1280–1282, Sep. 2011.

[27] D. Declercq and M. Fossorier, "Decoding algorithms for nonbinary LDPC codes over GF(q)," *IEEE Trans. Commun.*, vol. 55, no. 4, pp. 633–643, Apr. 2007.

[28] E. Arıkan, "Channel polarization: A method for constructing capacity-achieving codes for symmetric binary-input memoryless channels," *IEEE Trans. Inform. Theory*, vol. 55, no. 7, pp. 3051–3073, Jul. 2009.

[29] I. B. Djordjevic, H. G. Batshon, L. Xu, , and T. Wang, "Coded polarization-multiplexed iterative polar modulation (PM-IPM) for beyond 400 Gb/s serial optical transmission," *in Proc. Optic. Fiber Commun. Conf.*, Mar. 2010, OMK2.

[30] M. Arabaci, I. B. Djordjevic, L. Xu, and T. Wang, "Nonbinary LDPC-Coded modulation for high-speed optical fiber communication without bandwidth expansion," *IEEE Photonics Journal*, vol. 4, no. 3, pp. 728–734, Jun. 2012.

Lotfollah Beygi received his Ph.D. degree from Chalmers University of Technology, Göteborg, Sweden, in 2013. He was with the R&D division of Zaeim Electronic Industries from 2003 to 2008. Currently, he is with Qamcom Research & Technology AB. His main research interests include coded modulation and digital signal processing for fiber-optical and wireless communications.

Erik Agrell (M'99–SM'02) received the Ph.D. degree in information theory in 1997 from Chalmers University of Technology, Sweden.

From 1997 to 1999, he was a Postdoctoral Researcher with the University of California, San Diego and the University of Illinois at Urbana-Champaign. In 1999, he joined the faculty of Chalmers University of Technology, where he is a Professor in Communication Systems since 2009. In 2010, he cofounded the Fiber-Optic Communications Research Center (FORCE) at Chalmers, where he leads the signals and systems research area. His research interests belong to the fields of information theory, coding theory, and digital communications, and his favorite applications are found in optical communications.

Prof. Agrell served as Publications Editor for the IEEE Transactions on Information Theory from 1999 to 2002 and is an Associate Editor for the IEEE Transactions on Communications since 2012. He is a recipient of the 1990 John Ericsson Medal, the 2009 ITW Best Poster Award, the 2011 GlobeCom Best Paper Award, the 2013 CTW Best Poster Award, and the 2013 Chalmers Supervisor of the Year Award.

Joseph M. Kahn (M'90–SM'98–F'00) is a Professor of Electrical Engineering at Stanford University. His research addresses communication and imaging through optical fibers, including modulation, detection, signal processing and spatial multiplexing. He received A.B. and Ph.D. degrees in Physics from U.C. Berkeley in 1981 and 1986. From 1987-1990, he was at AT&T Bell Laboratories, Crawford Hill Laboratory, in Holmdel, NJ. He was on the Electrical Engineering faculty at U.C. Berkeley from 1990-2003. In 2000, he co-founded StrataLight Communications, which was acquired by Opnext, Inc. in 2009. He received the National Science Foundation Presidential Young Investigator Award in 1991. In 2000, he was elected a Fellow of the IEEE.

Magnus Karlsson received his Ph. D in 1994 from Chalmers University of Technology, Gothenburg, Sweden. Since 1995, he has been with the Photonics Laboratory at Chalmers, first as assistant professor and since 2003 as professor in photonics. He has authored or co-authored over 240 scientific journal and conference contributions in the areas of nonlinear optics and fiber optic transmission, and co-founded the Chalmers fiber-optic communication research center FORCE in 2010.

He has served in the technical committee for the Optical Fiber Communication Conference (OFC), and currently serves in the technical program committees for the European Conference of Optical Communication (ECOC), and the Asia Communications and Photonics Conference (ACP). He is associate editor for Optics Express since 2010.

He received the CELTIC excellence award in 2011, the best paper award at GlobeCom 2011, and was appointed Fellow of the Optical Society of America in 2012.